HHS Public Access

Author manuscript

Cancer Res. Author manuscript; available in PMC 2020 May 01.

Published in final edited form as:

Cancer Res. 2019 May 01; 79(9): 2392–2403. doi:10.1158/0008-5472.CAN-18-3024.

Spindle assembly checkpoint inhibition can resensitize p53-null stem cells to cancer chemotherapy

Changlong Liu, **Carolyn E. Banister**, and **Phillip J. Buckhaults**

Department of Drug Discovery and Biomedical Sciences, College of Pharmacy, University of South Carolina, Columbia, SC, USA, 29201

Abstract

TP53 mutations are common in most human cancers, but few therapeutic options for TP53-mutant tumors exist. To identify potential therapeutic options for cancer patients with TP53 mutations, we profiled 127 FDA approved chemotherapy drugs against human embryonic stem cells (hESC) in which we engineered TP53 deletion by genome editing. We identified twenty-seven cancer therapeutic drugs for which TP53 mutations conferred resistance; most of these drugs target DNA synthesis or topoisomerase and cause DNA damage. We then performed a genome-wide CRISPR/Cas9 knockout screen in the TP53-null hESC in the presence and absence of sublethal concentrations of cisplatin and identified 137 genes whose loss selectively re-sensitized the p53-null cells to this chemotherapeutic agent. Gene ontology classification of the resensitizing loci revealed significant overrepresentation of spindle checkpoint pathway genes. Moreover, we confirmed that targeting ZNF207/BuGZ sensitizes p53-null hESC to cisplatin. These data indicate that targeted inhibition of spindle assembly checkpoints (SAC) and chromosomal organizing centers may provide a way to treat p53-deficient cancer cells with standard chemotherapy drugs. Development of small molecule inhibitors of spindle assembly checkpoint proteins may be a useful strategy for rescuing DNA-damaging chemotherapeutics in TP53 mutant cancers.

Introduction:

The product of the TP53 gene is a sequence-specific DNA binding protein (p53) that regulates gene transcription. TP53 is one of the most well studied tumor suppressor genes, and is known be pivotal for cell cycle arrest, senescence, or apoptosis in response to DNA damage (1–4). In most human tumors, the p53 pathway is defective due in part to frequent (50%) occurrence of missense, nonsense, and frame-shift mutations that inactivate the transcriptional activation ability of p53 (5,6). Cancer associated somatic mutations in TP53 gene sometimes result in the accumulation of mutated p53 proteins, some of which may have dominant negative or gain of function activity. Most mutations result in in a complete loss of p53 protein, and in all cases, both alleles of p53 are altered and there is complete loss of normal p53 function in tumor cells (7). There is a significant association between p53 somatic mutations in tumors and the sensitivities of such tumors to cytotoxic drugs (8).

Corresponding Author: Phillip Joe Buckhaults, Department of Drug Discovery and Biomedical Sciences, College of Pharmacy, University of South Carolina, 715 Sumter Street, Columbia, SC 29208, USA. Phone: 803-777-3621; Fax: 803-777-8356;, phillip.buckhaults@gmail.com.

However, the ways in which p53 mutations cause drug resistance depends on the mode of action of the drug, other co-existing (and interacting) gene mutations, and perhaps the type of cancer (8,9).

The development of the CRISPR/Cas9 tool for genome editing has provided a more effective means to introduce targeted loss of functional mutations at specific sites within the genome (10,11). Functional genomic screens have been revolutionized by application of the CRISPR/Cas9 system, which allows efficient and specific genome engineering in mammalian cells and several studies have used pooled sgRNA libraries for genome-wide loss-of-function (12–17). The observation that BRCA1 and BRCA2 deficient cells are sensitive to inhibitors of poly (ADP-ribose) polymerase (PARP) has spurred the development of screens for additional examples of gene synthetic lethality to target deficiencies in different type of cancers(18,19).

We sought to use CRISPR/Cas9 synthetic lethal interaction screening technology to identify specific targets that would enable more effective treatment of drug-resistant p53-null tumors. We created TP53 knockout derivatives of human embryonic stem cells, performed drug sensitivity screening on 127 FDA approved cancer therapeutics to identify TP53 mutation associated resistance, and then performed a pooled CRISPR/Cas9 library knockout screen on TP53 knockout hESC lines in the absence and presence of sub lethal concentration of cancer chemotherapy drug, and identified genes that, when disrupted by CRISPR/Cas9 editing, resensitized the p53-null, drug-resistant cells to the chemotherapy. We found that Cisplatin resistant p53-null embryonic stem cells could be re-sensitized to Cisplatin by inhibiting genes that regulate cell spindle assembly checkpoints (SAC) and chromosomal organizations.

Materials and Methods

Cell lines culture

Human H9 ESCs (Lot No.: WIC-WA09-MB-001, WiCell, Wisconsin) and its derivatives were maintained at 37 °C, 5% CO2 in chemical defined medium TeSR-E8 medium (Stemcell Tech.) with 100U/ml penicillin & 100 μg/ml streptomycin (Gibco) on matrigel (#CB40230A, Corning) coated tissue culture vessels. Authentication of H9 ESCs were performed by WiCell. ESCs were passaged every 4 to 6 days to maintain sub-confluence using 0.5 mM EDTA as described previously (20). Human colon cancer RKO cells (kindly given by Dr. Bert Vogelstein) and its derivatives were maintained at 37 °C, 5% CO2 in McCoy's 5A media (Fisher) supplemented with 10% FBS and 100U/ml penicillin & 100 μg/ml streptomycin (Gibco). RKO cells were passaged every 3 to 4 days to maintain sub-confluence (Authentication of RKO cell line was performed by JHU-GRCF Biorepository & Cell Center). Cells were screened for mycoplasma before experiments using a MycoAlert™ Mycoplasma Detection Kit (Lonza).

All cell lines were passaged in our laboratory for no more than 30 passages after resuscitation.

TP53 knock out in human embryonic cells and RKO cells with CRISPR/Cas9

TP53 knockout hESCs and RKO cells were generated using CRISPR/Cas9 as described previously (21) with minor modifications. Briefly, human codon-optimized Streptococcus pyogenes wild type Cas9 (Cas9–2A-GFP) was obtained from Addgene (#44719). Chimeric guide RNA expression cassettes with different small guide RNA, TP53_Up_sgRNA: 5'-CCATTGTTCAATATCGTCCG −3' and TP53_Down_sgRNA: 5'-GGGCAGCTACGGTTTCCGTC −3' were ordered as gBlock. These gBlocks were amplified by PCR using primers: gBlock_Amplifying_F: 5'-TGTACAAAAAAGCAGGCTTTAAAGG-3' and gBlock_Amplifying_R: 5'-TAATGCCAACTTTGTACAAGAAAGC-3'. The PCR product was purified by Agencourt Ampure XP PCR Purification beads according to manufacturer's protocol (Beckman Coulter). 1.5 μg of Cas9 plasmid and 0.5 μg of each gRNAgBlock were co-transfected into hESCs via Lipofectamine 3000 (Thermo Fisher Scientific). For TP53-KO hESCs, the transfected cells were cultured in TeSR-E8 medium with 1 μM Nutlin-3a for one week. For TP53-KO RKO cells, single clones were picked up and validated by PCR and Western blotting.

Cell viability assay

NCI Approved Oncology Drug Set IV containing 127 FDA-approved anticancer drugs was obtained from the NCI under a material transfer agreement. The full list of drugs is shown in supplementary Table S1. TP53 knockout or wild-type human ES cells were seeded in 96-well microplates in E8 medium with 6,000 cells per well that would reach about 85% confluent at the end of the assay. Human ES cells were plated one day before treatment with a 7-point twofold dilution series (starting with 10 μM) of each compound or solvent (dimethyl sulfoxde, DMSO or Dimethylformanide, DMF) control. After 72 hrs incubation, cells were stained with 35 μM resazurin (Sigma), then quantification of fluorescent signal intensity was performed on Thermo Fluorskan Ascent plate reader at excitation and emission wavelengths of 544/590 nm. Data were normalized to the solvent control (DMSO or DMF) group. The area under a curve (AUC) was calculated using *auc* function (flux package) in R (www.r-project.org). The two-side t-test was performed with *t.test* function in R. The hierarchical clustering analysis of drugs AUC pattern in different samples was carried out using heatmap.2 function (gplots package) in R (All R code available after request). Viability response curves of Cisplatin and Paclitaxel on TP53-KO hESCs or RKO cells were generated using drc package (Analysis of Dose-Response Curves) in R.

Lentiviral CRISPR library amplification and cell transduction

The human GeCKO lentiviral library lentiCRISPRv2 (22) in one plasmid was bought from Addgene (cat # 1000000048) as library A and library B. The library was amplified in accordance to the author's recommendations. Briefly, 2 μL of the 50 ng/uL lentiCRISPRv2 plasmid was electroporated with 25 μl of the Lucigen Endura electro competent cells (cat #60242) in 1.0 mm cuvette using a GenePulser Xcell (Bio-Rad) apparatus at the following settings: 10 μF capacitance, 600 Ω resistance, 1800 V. Then transfer cells were placed in recovery medium to the final volume of 1 ml, and the above procedure was repeated for a total of 4 electroporations for each module of the lentiCRISPRv2. The recovered

transformed bacteria in 4 ml medium were incubated at 250 rpm at 37 °C for 1 h, and plated onto pre-warmed twenty 10 cm dishes with Ampicillin LB-agar for 14 hours at 32 °C. The grown colonies were recovered from the plates by pipetting/scrapping in LB-broth. The plasmid DNA from transformed cells was purified using QIAfilter Plasmid Maxi Kit (Qiagen).

For lentiviral production, the day before transfection, 293T cells were seeded at 1.2×10^7 cells per 150-cm^2 dish. On the next day, sixty micrograms plasmid DNA was used for transfection of one 150 mm dish. The DNA cocktail contained 10.5 μg envelope-coding plasmid pMD.G, 19.5 μg of the packaging plasmid pSPAX2 and 30 μg of transgene vector plasmid by CaCl2 method according to procedure published. Next day the culture medium was replaced, and cells were grown for another 48 h. Supernatants from the twenty 150-mm dish with transfected 293T cells were harvested, combined and clarified through a 0.45 μm cellulose acetate filter (Millipore, Cat.No: SCHVU01RE). Then the virus supernatants concentrated using PEG6000 and concentrated virus were stored in −80 °C freezer.

GeCKO CRISPR library screening

Viral transduction was carried out through spinfection with an MOI of 0.3 to assure that no more than 1 viral particle enters a given cell. The spinfection was conducted for 2 hours at 1000 ×g and 37°C and then incubated overnight a 37°C. Cells were trypsinized and transferred to matrigel coated 150-mm culture dishes containing growth media plus 0.4 μM puromycin (Sigma) to select for successful transduction. After 3 days of selection all remaining cells should be successfully transduced, these cells were then collected and plated. The lentiviral construct will insert a copy of the puromycin resistance, a single sgRNA and Cas-9 genes into the cells DNA through retroviral activity, allowing the transduced cells to pass the resistance and CRISPR activity to all daughter cells. This protocol was conducted using 1.1×10^8 starting cells to give ~200 fold coverage of the library A and B, respectively. After selection, survived cells were divided into two parts. One part (> 20 million) was treated with 200 nM Cisplatin. Another part (> 20 million) was treated with control DMF. Cells were passaged after reaching 90% confluence. After about 14 doublings, cells were then collected for DNA extraction.

DNA extraction and sequencing

DNA was extracted from cell trypsinate using Blood & Cell Culture DNA Midi kit (Qiagen). The sgRNA sequences present in the collected DNA were amplified through PCR using primers that attach Illumina sequencing recognition sites and barcodes. A total of 100 μg of genomic DNA template was used per sample.

For each sample, we performed 25 separate 100 μl reactions with 4 μg genomic DNA in each reaction using KAPA Real-time Library Amplification Kit (KAPA Biosystems) and then combined the resulting amplicons. Primers sequences to amplify lentiCRISPR sgRNAs for PCR are

Forward primer for PCR:
AATGATACGGCGACCACCGAGATCTACACTCTTTCCCTACACGACGCTCTTCCGAT

CTNNNNNTCTTGTGGAAAGGACGAAACACCG. (NNNNN: variable base sequence to introduce diversity).

Reverse primer:

CAAGCAGAAGACGGCATACGAGATNNNNNNGTGACTGGAGTTCAGACGTGTGCT CTTCCGATCTTGTGGGCGATGTGCGCTCTG. (NNNNNN: Sample Barcode).

Sequencing primer: ACACTCTTTCCCTACACGACGCTCTTCCGATCT

The PCR product was purified using the Agencourt AMPure XP bead bound purification kit. The purified PCR product was then sequenced on an Illumina HiSeq 2500.

Data processing and analysis

The Illumina NextSeq raw FASTQ files were processed by MAGeCK software (23) with default parameters using sgRNA sequences list for all genes from the GeCKO v2 library A and B to produce raw counts tables. The numbers of uniquely aligned reads for each library sequences were calculated. Then the numbers of reads for each unique sgRNA for a given sample were normalized as following. sgRNA counts from GeCKO library A and B were merged after normalization.

$$\text{normalized reads per sgRNA} = \frac{\text{reads per sgRNA}}{\text{total reads for all sgRNA in sample}} \times 10^6 + 1$$

For negative selection analysis, MAGeCK-RRA was used as the MAGeCK analysis pipeline. The output file with gene summary was used for downstream analysis. Gene ontology analysis for overrepresented genes was performed using R package clusterProfiler (24).

For each gene in each sample, we defined its CRISPR score (25) as the average log2 fold-change in the abundance of all single guide sgRNAs targeting the gene after 14 population doublings (26).

$$\text{CRISPR gene score (25)} = \text{average}\left[\log 2\left(\frac{\text{End sgRNA abundance}}{\text{Initial sgRNA abundance}}\right)\right]$$

The cell-essential genes are involved in fundamental biological processes. Gene set enrichment analysis was performed on genes ranked by CRISPR gene score.

Validation of spindle assembly checkpoint gene ZNF207/BuGZ

Human TP53 knockout embryonic stem cells were infected at low MOI by virus produced using pCLIP-Cas9-Nuclease-EFS-Blast (TransOMIC) and selected using blastcidin (10 μg/ml). The stable Cas9-expressing TP53-KO hESCs were infected with viruses with two sgRNAs against gene ZNF207/BuGZ (#TEDH-1090944, TransOMIC) or control gene OR1C1 (#TEDH-1055091, TransOMIC). These two sgRNAs could induce fragment deletion. We treated these cells with either 200 nM Cisplatin or vehicle DMF. We used realtime quantitiative PCR to quantify the ZNF207 knockout locus, using gRNA flanking

primers that only amplify when the intervening sequence has been deleted. ZNF207-KO-F1: GGTTGGGAAAGTGAGGGATT; ZNF207-KO-R1: AACACTTCTCACAGGAACTTGC. OR1C1-KO-F1: CAGCCTCCTTCTGTGTGTGA. OR1C1-KO-R1: TGCTTGCCCTGAGTAGAGGT

The total genomic DNA was monitored by LINE gene using LINE primer: LINE-F: AAAGCCGCTCAACTACATGG; LINE-R: CTCTATTTCCTTCAGTTCTGCTC. The relative percentage of ZNF207 or OR1C1 knockout cell number was defined as: $2^{-\Delta CT(\text{Gene}-\text{LINE})}/2^{-\Delta CT(\text{Gene}-\text{LINE})\text{ at Day0}}$.

Drug synergy experiment and analysis

A Paclitaxel and Cisplatin drug matrix (12 × 8) in a 96-well plate was made for drug synergy experiment. Paclitaxel on row was an 11-point 2-fold dilution series with starting concentration of 0.0016 μM and Cisplatin on column was a 7-point 2-fold dilution series with starting concentration of 2 μM, 5000 TP53-KO hESCs per well or 2000 TP53-KO RKO cells per well were plated on three 96-well plates one day before treatment with Paclitaxel and Cisplatin drug matrix. After 72 hrs incubation for TP53-KO hESCs and 96 hrs incubation for TP53-KO RKO cells, cells were stained with 35 μM resazurin (Sigma), then quantification of fluorescent signal intensity was performed on Thermo Fluorskan Ascent plate reader at excitation and emission wavelengths of 544/590 nm. The drug synergy score were evaluated using ZIP model (Zero Interaction Potency model) in synergyfinder package(27).

Immunostaining and microscopy

Cells were fixed in 4% paraformaldehyde in DPBS and incubating for 20 minutes at room temperature. After washing 3 times with DPBS, the cells were permeabilized and blocked with blocking buffer (0.1% Triton-X 100 and 10% FCS in DPBS) for 1 hour at room temperature, and then incubated with primary antibodies in blocking buffer. Anti-Oct4 (1:2000, cat#:561555, BD Pharmingen™), anti-Nanog (1 : 100, cat#: 560109, BD Pharmingen™) and anti-Sox2 (1 : 100, cat#: 561469, BD Pharmingen™) antibodies overnight at 4C. Then they were incubated with secondary antibodies; anti-rabbit IgG, anti-mouse IgG or anti-mouse IgM conjugated with Alexa 488 (1: 1000, cat#: A11004, Invitrogen) or Alexa 568 (1: 1000, cat#: A10667, Invitrogen) in blocking buffer for 1 h at room temperature. The cells were counterstained with 4, 6-diamidino-2-phenylindole (DAPI) for 10 minutes. Images were taken using microscope equipped with monochrome EMCCD camera.

Western blotting analyses

Cell lysates were prepared using RIPA buffer (150mM NaCl, 1% Triton X-100, 0.5% sodium deoxycholate, 0.1% SDS and 50mMTris-HCl, pH 8.0), supplemented with protease inhibitor cocktail (cat#: P8340, Sigma). The concentration of protein was determined using Pierce BCA Protein Assay Kit (cat#: 23227, Thermo Scientific). 20 ug of denatured cell lysates were separated by electrophoresis on 10% or/and 7% SDS-PAGE, and then were transferred to hydrophobic PVDF. The blot was blocked with TBST (10mMTris-HCl, pH 7.5, 150 mM NaCl, and 0.1% Tween-20) containing 5% non-fat dry milk followed by an

overnight incubation with primary antibody in TBST at 4 °C overnight. After washing with TBST, the membrane was incubated with horseradish peroxidase (HRP)-conjugated secondary antibody for 1 hour at room temperature with constant agitation. Signals were raised with SuperSignal™ West Pico Chemiluminescent substrate (cat#: 34077, Thermo Scientific) and detected using a ChemiDoc™ MP imaging system (Bio-RAD). Primary antibodies for p53 (1:400, cat#: sc-126, Santa Cruz), β-actin (1:1,000, cat#: 4970, CST) and horseradish peroxidase linked secondary antibodies for mouse IgG (1:2,000, cat#: 7076, CST) and rabbit IgG (1:2,000, cat#: 7074, CST) were used.

Statistical analyses

We evaluated the data by unpaired *t*-test (student *t*-test) using the GraphPad Prism software (GraphPad Software, Inc), and values of $P < 0.05$ were considered to be significant (indicated by asterisks in figures). The error bars represent the standard deviation (S.D.).

Results:

Generating and characterizing TP53 knockout derivatives of human ESCs.

In order to screen for p53 dependent drug sensitivity, without confounding interactions from other gene mutations, we chose the human embryonic stem cell line E9 (hESC), which is wild-type for TP53 (TP53-WT) and it has few known acquired gene mutations. Embryonic stem cells are also a reasonable model for cancer stem cell biology. We constructed TP53 knockout (TP53-KO) derivatives of hESCs using CRISPR/Cas9 genome editing, targeting two locations within exon 2 of the TP53 gene (Figure 1A). gBocks encoding two small guide RNAs (sgRNA) were co-transfected with Cas9 vector into human ES cells, and TP53 defective cells were selected by growing the cells in the presence of 1 μM Nutlin-3a, which is an MDM2 inhibitor and potent activator of p53-induced arrest and apoptosis (25). TP53-KO hESCs retained morphology similar to their parental TP53 wild-type hESCs (Fig. 1A). TP53 gene locus of TP53-KO hESCs were confirmed by DNA sequencing and the transcriptional level of TP53 was abolished in TP53-KO hESCs compared to TP53-WT hESCs (Supplementary Fig. S1). The p53 protein was visualized in the parental TP53-WT hESCs by Western blotting, and the absence of p53 protein was confirmed in TP53-KO hESCs (Fig. 1A). Furthermore, to determine if loss of p53 affected the pluripotency of embryonic stem cells, we performed immuno-staining of TP53 WT and KO hESCs for pluripotent markers OCT4, SOX2 and NANOG. Both the TP53-WT parental hESCs and the TP53-KO hESCs express these pluripotent stem cell markers (Fig. 1B) suggesting that TP53-KO hESCs were still phenotypically embryonic stem cells. We observed a modest increase in the rate of cell proliferation in the TP53-KO hESCs compared to TP53-WT hESCs (Fig. 1C). Finally, as expected, TP53-KO hESCs are resistant to the growth inhibitory effects of Nutlin-3a whereas the TP53-WT hESCs are severely growth arrested at very low concentrations of Nutlin-3a (Fig. 1D).

Loss of p53 function confers resistance to multiple cancer chemotherapy drugs in human embryonic stem cells

Many clinical studies have demonstrated the prognostic relevance of mutated p53, often associating mutant TP53 with resistance to alkylating agents, anthracyclines,

antimetabolites, anti-estrogens and EGFR-inhibitors (8). To establish a cause and effect relationship between p53 inactivation and resistance to specific chemotherapies, we screened the NCI Approved Oncology Drug Set IV, which is a panel of 127 FDA-approved anticancer drugs (Supplementary Table S1) against TP53-WT and TP53-KO hESCs and determined which drugs were less effective after mutational inactivation of p53. Dose-response measurements were performed in experimental triplicates and the effects of 72 h of drug treatment on hESC viability was measured using a fluorescent resazurin cell viability assay. The area under the curve (AUC) was used to quantify the sensitivity of each cell line to each drug. Unsupervised hierarchical clustering via the AUC measurements drove the 127 drugs into three distinct groups: (I) drugs for which TP53-KO hESCs are more resistant to TP53-KO hESCs than TP53-WT hESCs; (II) drugs for which both TP53-WT and TP53-KO hESCs are equally sensitive; and (III) drugs for which both TP53-WT and TP53-KO hESCs are resistant (Fig. 2A). We found that 27 drugs were significantly different between TP53-WT and TP53-KO hESCs, and all drugs were less effective on the TP53-KO derivatives than the TP53-WT parental hESCs (Fig. 2B and Supplementary Table S2). These 27 p53-null hESCs resistant drugs can be classified according to their therapeutic targets (28) and most of these drugs inhibit DNA synthesis and/or topoisomerase (Fig. 2C).

TP53 loss causes resistance to Irinotecan, Oxaliplatin, Cisplatin and Olaparib

From the initial screen, we chose ten drugs that are commonly used for the clinical management of colorectal or epithelial ovarian cancer (Fig. 3A) and Nutlin-3a as a control (Fig. 3B), and further confirmed that some of these drugs are ineffective against TP53-KO hESCs. The standard approach for epithelial ovarian chemotherapy is the combination of a platinum compound, such as Cisplatin or Carboplatin, and a taxane, such as Paclitaxel or Docetaxel. Olaparib, a PARP inhibitor, is used to treat women with advanced ovarian cancer who have BRCA1 or BRCA2 gene mutations. TP53-KO human ES cells were resistant to Cisplatin (Fig. 3C), Olaparib (Fig. 3D) and Carboplatin (Fig. 3E) whereas TP53-WT human ES cells were very sensitive to these drugs at low concentration. Both TP53 KO and WT were sensitive to Docetaxel (Fig. 3F) and Paclitaxel (Fig. 3G) at all tested concentrations.

Colorectal cancer is often treated with 5-fluorouracil, Capecitabine, Irinotecan, Oxaliplatin and Trifluridine. Our result showed that TP53-KO hESCs were resistant to Irinotecan (Fig. 3H), Oxaliplatin (Fig. 3I) and Trifluridine (Fig. 3J) whereas TP53 wild type hESCs were very sensitive to Irinotecan and Oxaliplatin at low concentration (0.16 uM) and both TP53-KO and WT hESCs were resistant to Capecitabine (Fig. 3K). Also, both TP53-KO and WT human ES cells were resistant to Fluorouracil at low concentrations (Fig. 3L). However, TP53-WT human ES cells were sensitive to Fuorouracil at high concentrations (Fig. 3L). These results suggest that a combination of both p53 dependent and p53 independent classes of drugs for chemotherapy may be more helpful to cure cancer patients.

CRISPR/Cas9 Knockout Library screening to resensitize p53-null hESCs to Cisplatin.

We determined the optimal concentration of Cisplatin at which TP53-WT hESCs were very sensitive, yet TP53-KO hESCs were very resistant (200nM). We screened TP53-KO hESCs in the absence and presence of 200nM Cisplatin, to search for knockouts that would resensitize the hESCs to low concentrations of cisplaitn. Lentiviral transductions were

performed at a MOI of 0.3 to make it likely that only one sgRNA virus infected per transduced cell. Sufficient cells were transduced to allow 200× coverage of each sgRNA within the library. Cells were selected for stable viral integration with puromycin for 3 days and then passaged for 14 doublings in either DMF vehicle or Cisplatin at 200 nM. At least 200× library coverage was maintained by plating > 20 million cells per passage. After 14 doublings the cells were collected and genomic DNA was extracted. Lentiviral sgRNA constructs were amplified by PCR and quantified by deep sequencing (Fig. 4A). For each human gene represented in the GECKO v2 library, we defined its CRISPR gene score (25) as the average over all guides for a given gene of the log2 fold changes in the abundances of each single guide sgRNAs targeting the given gene after about 14 population doublings. As a positive control for the screen performance, we evaluated the CRISPR gene scores for previously published 1,580 essential genes and 927 nonessential genes (16,29) and the 2,000 non-targeting control sgRNAs that are included in the GeCKO library. As expected, the CSs of essential and nonessential genes were significantly different (Fig. 4B), indicating that essential genes were indeed depleted during the screen, independent of the presence or absence of Cisplatin. We performed gene set enrichment analysis (GSEA) on all genes ranked ordered by CS, in order to agnostically group the depleted genes according to functional categories. Consistent with prior work, essential genes involving in fundamental cellular processes such as ribosome function and protein translation were strongly depleted both in control DMF (vehicle) and in Cisplatin treated cells (Fig. 4C). These results indicated that the CRISPR screens on TP53-null hESCs with DMF or Cisplatin were valid.

Gene knockouts causing chromosome missegregation can resensitize TP53-null human ESCs to Cisplatin

To identify genes that could resensitize TP53 knockout cells to Cisplatin, the sgRNAs counts from drug vs vehicle screens were analyzed using Model-based Analysis of Genome-wide CRISPR/Cas9 Knockout (MAGeCK) method (21). MAGeCK algorithm identifies both positively and negatively selected genes simultaneously and reports robust results across different experimental conditions. MAGeCK analysis identified 137 genes significantly depleted ($p < 0.01$) (Supplementary Table S3) in Cisplatin treatment but not in DMF treatment (Fig. 5A). Consistent with MAGeCK analysis, inspection of the CS for these genes confirmed that all have lower CS in Cisplatin treatment than that in DMF control (Fig. 5B). We also manually inspected the individual sgRNAs and found that the abundances of all of the the sgRNAs targeting the same gene were depleted in Cisplatin treatment compared to that in DMF control (Fig. 5C, 6 sgRNAs targeting gene ZNF207/BuGZ or BRD7 are shown). We next performed GO pathway analysis of all 137 significantly depleted genes and found that spindle assembly checkpoint, chromosome organization and chromatid separation genes were overrepresented among the top 20 significantly enriched GO terms (Fig. 5D and Table 1).

To functionally test one of the identified spindle assembly checkpoint genes, ZNF207/BuGZ, we generated lentivirus with two sgRNAs against gene ZNF207/BuGZ and transduced them into stable Cas9-expressing TP53-KO hESC line. We treated these cells with either 200 nM Cisplatin or vehicle DMF for ten days, isolated genomic DNA at day 6 and 10, and we used realtime qPCR to quantify the ZNF207/BuGZ knockout locus, using

gRNA flanking primers that only amplify when the intervening sequence has been deleted (Supplementary Fig. S2). The ZNF207/BuGZ knockout cells were depleted in both Cisplatin and control cells (consistent with it being an essential gene) however ZNF207/BuGZ knockout cells were depleted faster in the presence of Cisplatin than in the presence of DMF vehicle control (Fig. 5E). Moreover, we generated two more TP53-KO hESC lines and validated the effect of Cisplation on these two hESCs lines with ZNF207/BuGZ knockout. The results showed that ZNF207/BuGZ knockout cells were more sensitive to Cisplatin (Supplementary Fig. S3). Furthermore, we examined ZNF207 gene expression from ovarian cancer patients in published datasets with clinical outcome information (patients with all stages and received chemotherapy that contained platin) and noted that loss of ZNF207 expression predicted good response to chemotherapy containing platinum compound in TP53-mutated ovarian cancer. However, there is no significant difference in TP53 wild type ovarian cancer (Figure 5F and 5G). These results suggest that genes involving in chromosome missegregation are associated with Cisplatin sensitivity on TP53-null hESCs and that pharmacological inhibitors that can be titrated may reveal a therapeutic window for sensitizing TP53 mutant cancer cells to Cisplatin. We also validated the effect of CDK9 and KDM1A gene knockout in TP53-KO hESCs in response to Cisplatin. But the difference is not significant. Furthermore, we examine CDK9 and KDM1A gene expression from ovarian cancer patients in published datasets with clinical outcome information. Interestingly, we found that both loss of CDK9 and KDM1A expression predicted good responses to chemotherapy containing platinum compound in TP53-mutated ovarian cancer (Supplementary Figure S4).

Chromosome missgregation by Paclitaxel could sensitize TP53-KO hESCs and TP53-KO colon cancer cells to Cisplatin

It has been reported that targeting ZNF207/BuGZ could cause chromosome misalignment due to defective interactions between microtubule and kinetochores (30). Paclitaxel could stabilize the microtubule polymer and protects it from disassembly lead to defects in mitotic spindle assembly, chromosome segregation, and cell division. We performed drug synergy experiment using low concentration of Paclitaxel and Cisplatin. The inhibition of Cisplatin on TP53-KO hESCs was increased by Pacliatxel (Fig. 6A). To further validation our findings on human ESCs, We generated two clones of TP53 knockout RKO cells using CRISPR/Cas9 (Supplementary Fig. S5). Like human TP53-KO ESCs, TP53-KO RKO cells are resistant to Cisplatin compared to TP53-WT RKO cells (Supplementary Fig. S5). Then we performed a drug synergy experiment in human colon cancer RKO cells using Cisplatin and Paclitaxel. The inhibition of Cisplatin on TP53-KO RKO cells was increased greatly by Pacliatxel (Fig. 6B and 6C).

Discussion

There are several recent studies using CRISPR dropout screening to identify essential fitness genes and/or gene synthetic lethality with cancer cells lines (14,16,17,26,31). However, cancer cell lines have a tremendous number of gene mutations and amplifications, some of which were acquired in culture and are not common in human cancers, that could confuse screening outcomes when studying the effects of a single gene loss (32,33). For this reason,

in this work, we chose to use human embryonic stem cells to study drug resistance and genome-wide CRISPR/Cas9 screening for gene knockouts that could resensitize chemotherapy resistant cells. We generated TP53 knockout human embryonic stem cells and then investigated the sensitivities to 127 FDA approved cancer chemotherapy drugs, identifying 27 drugs for which p53 mutations cause drug resistance. We then performed genome-wide CRISPR screening of the p53 null cells in the presence of a sublethal concentration of the chemotherapy drug Cisplatin, and identified 137 novel genetic perturbations that cause re-sensitization of TP53-null cells to the chemotherapy.

During cancer cell development, the epigenetic status of cancer cells are often altered in ways such that cancer cells either acquire or inappropriately maintain stemness and pluripotency. Several studies have identified an embryonic stem cell-like gene expression signature in breast cancer (34) and in poorly differentiated aggressive human tumors (35), and such stem like signatures usually correlate with poor prognosis. Our previous study proved that repressing stemness by epigenetic means can inhibit colorectal tumor organoid proliferation in 3D culture system(21). We have also investigated p53 dependency of drug sensitivity in human colorectal cancer cell lines with and without TP53 deletions, and found that most of drugs have similar response patterns to what we report here in human embryonic stem cells (Supplementary Fig. S5A and S5D) and indicated that embryonic stem cell lines are good tools to study p53 dependence of drug sensitivity.

Chemotherapy resistance is a major problem in the clinical management of cancer patients. Drug resistance may arise due to intrinsic cellular resistance that is mediated through ATP-dependent membrane transporters, nuclear receptors, or by inhibiting drug accumulation or stimulating drug metabolism and inactivation (36–38). Inactivation of TP53 has been shown to result in resistance to chemotherapeutic drugs by abrogating p53-dependent apoptosis (39). In our study, we proved that TP53 mutation causes resistance to 27 drugs in human embryonic stem cells. Most of these drugs inhibit DNA synthesis and/or topoisomerase as their primary therapeutic targets (28).

P53 can prevent chromosomal instability through its ability to eliminate cells that are at risk of aberrant mitoses(40,41). Studies suggest that p53-deficient cells are better at tolerating genetic stress produced by aberrant gene dosage (42,43). Hence, the absence of p53 allows both the accumulation and survival of aneuploid cells. Aneuploidy is a common characteristic of most cancer cells and has been suggested as a contributor to tumorigenesis (44). It has been reported that PLK1, a mitotic kinase, as a resistance mediator whose genomic as well as pharmacological inhibition restored drug sensitivity to trastuzumab emtansine (T-DM1) in HER2-positive breast cancer. The T-DM1 sensitization upon PLK1 inhibition was initiated by a spindle assembly checkpoint (SAC)-dependent mitotic arrest, leading to caspase activation, followed by DNA damage through CDK1-dependent phosphorylation and inactivation of Bcl-2/xl (45,46). Interestingly, up-regulation of PLK1 control the G2/M transition in the colorectal cancer RKO cells whose TP53 genes were inactivated and p53 inactive RKO cells were highly sensitive to PLK1 inhibitors (47). Additionally, missegregation of large numbers of chromosomes due to complete inactivation of the mitotic checkpoint results in cell death in human cancer cells(48,49). Our CRISPR screening on human p53-null embryonic stem cells indicated that cells are made more

sensitive to Cisplatin by loss of spindle assembly checkpoints (SAC) and other chromosomal segregation genes in context of absence of p53. Cisplatin causes increased genetic instability, which may synergize with p53 and spindle checkpoint absence. Loss of p53 induces genomic instability and helps cells acquire additional driver events that accelerate transformation, metastasis, and drug resistance (50). Dysfunction of spindle assembly checkpoints and/or chromosomal organization facilitates aneuploidy to enable cells to survive moderate levels of genetic instability. Finally, in this background, high levels of genetic instability caused by the addition of chemotherapeutic agents such as Cisplatin may result in decreased survival due to catastrophic genetic damage and cell death (Fig. 6D)(44).

In conclusion, we generated a human TP53 knock out embryonic stem cells and did drug screening of 127 FDA approved drugs on it. There are 27 drugs are associated with p53 status and most of these resistant drugs inhibit DNA synthesis and topoisomerase based on their therapeutic targets. Furthermore, we performed a genome-wide CRISPR screening on TP53 knock out embryonic stem cells with drugs and found p53-null embryonic stem cells could be resensitized to Cisplatin by inhibiting genes that regulate cell spindle assembly checkpoint (SAC) and chromosomal organizations. Our finding could provide a new way to treat p53-deficient cancer cells with standard chemotherapy drugs.

Supplementary Material

Refer to Web version on PubMed Central for supplementary material.

Acknowledgements

We thank the Microscopy and Flow Cytometry Core Facility of College of Pharmacy at University of South Carolina for microscopy, and all members in Dr. Phillip Buckhaults laboratory for this manuscript proof reading. This work was supported by NIH Grant U01 CA158428 (to P.J.B.).

Disclosure of Potential Conflicts of Interest: Dr. Phillip J. Buckhaults reports receiving a commercial research grant from Janssen Research and Development. No potential conflicts of interest were disclosed by other authors.

Reference:

1. Kastenhuber ER, Lowe SW. Putting p53 in Context. Cell 2017;170:1062–78 [PubMed: 28886379]
2. Levine AJ. p53, the cellular gatekeeper for growth and division. Cell 1997;88:323–31 [PubMed: 9039259]
3. Vousden KH, Lu X. Live or let die: the cell's response to p53. Nat Rev Cancer 2002;2:594–604 [PubMed: 12154352]
4. Williams AB, Schumacher B. p53 in the DNA-Damage-Repair Process. Cold Spring Harb Perspect Med 2016;6
5. Brosh R, Rotter V. When mutants gain new powers: news from the mutant p53 field. Nat Rev Cancer 2009;9:701–13 [PubMed: 19693097]
6. Shetzer Y, Solomon H, Koifman G, Molchadsky A, Horesh S, Rotter V. The paradigm of mutant p53-expressing cancer stem cells and drug resistance. Carcinogenesis 2014;35:1196–208 [PubMed: 24658181]
7. Giacomelli AO, Yang X, Lintner RE, McFarland JM, Duby M, Kim J, et al. Mutational processes shape the landscape of TP53 mutations in human cancer. Nat Genet 2018
8. Hientz K, Mohr A, Bhakta-Guha D, Efferth T. The role of p53 in cancer drug resistance and targeted chemotherapy. Oncotarget 2017;8:8921–46 [PubMed: 27888811]

9. Marin JJ, Romero MR, Martinez-Becerra P, Herraez E, Briz O. Overview of the molecular bases of resistance to chemotherapy in liver and gastrointestinal tumours. Curr Mol Med 2009;9:1108–29 [PubMed: 19747110]
10. Cong L, Ran FA, Cox D, Lin S, Barretto R, Habib N, et al. Multiplex genome engineering using CRISPR/Cas systems. Science 2013;339:819–23 [PubMed: 23287718]
11. Mali P, Yang L, Esvelt KM, Aach J, Guell M, DiCarlo JE, et al. RNA-guided human genome engineering via Cas9. Science 2013;339:823–6 [PubMed: 23287722]
12. Shalem O, Sanjana NE, Hartenian E, Shi X, Scott DA, Mikkelsen TS, et al. Genome-scale CRISPR-Cas9 knockout screening in human cells. Science 2014;343:84–7 [PubMed: 24336571]
13. Wang T, Wei JJ, Sabatini DM, Lander ES. Genetic screens in human cells using the CRISPR-Cas9 system. Science 2014;343:80–4 [PubMed: 24336569]
14. Shalem O, Sanjana NE, Hartenian E, Shi X, Scott DA, Mikkelson T, et al. Genome-scale CRISPR-Cas9 knockout screening in human cells. Science 2014;343:84–7 [PubMed: 24336571]
15. Chen S, Sanjana NE, Zheng K, Shalem O, Lee K, Shi X, et al. Genome-wide CRISPR screen in a mouse model of tumor growth and metastasis. Cell 2015;160:1246–60 [PubMed: 25748654]
16. Hart T, Chandrashekhar M, Aregger M, Steinhart Z, Brown KR, MacLeod G, et al. High-Resolution CRISPR Screens Reveal Fitness Genes and Genotype-Specific Cancer Liabilities. Cell 2015;163:1515–26 [PubMed: 26627737]
17. Wang T, Birsoy K, Hughes NW, Krupczak KM, Post Y, Wei JJ, et al. Identification and characterization of essential genes in the human genome. Science 2015;350:1096–101 [PubMed: 26472758]
18. Farmer H, McCabe N, Lord CJ, Tutt AN, Johnson DA, Richardson TB, et al. Targeting the DNA repair defect in BRCA mutant cells as a therapeutic strategy. Nature 2005;434:917–21 [PubMed: 15829967]
19. Bryant HE, Schultz N, Thomas HD, Parker KM, Flower D, Lopez E, et al. Specific killing of BRCA2-deficient tumours with inhibitors of poly(ADP-ribose) polymerase. Nature 2005;434:913–7 [PubMed: 15829966]
20. Beers J, Gulbranson DR, George N, Siniscalchi LI, Jones J, Thomson JA, et al. Passaging and colony expansion of human pluripotent stem cells by enzyme-free dissociation in chemically defined culture conditions. Nat Protoc 2012;7:2029–40 [PubMed: 23099485]
21. Liu C, Banister CE, Weige CC, Altomare D, Richardson JH, Contreras CM, et al. PRDM1 silences stem cell-related genes and inhibits proliferation of human colon tumor organoids. Proc Natl Acad Sci U S A 2018;115:E5066–E75 [PubMed: 29760071]
22. Sanjana NE, Shalem O, Zhang F. Improved vectors and genome-wide libraries for CRISPR screening. Nat Methods 2014;11:783–4 [PubMed: 25075903]
23. Li W, Xu H, Xiao T, Cong L, Love MI, Zhang F, et al. MAGeCK enables robust identification of essential genes from genome-scale CRISPR/Cas9 knockout screens. Genome Biol 2014;15:554 [PubMed: 25476604]
24. Yu G, Wang LG, Han Y, He QY. clusterProfiler: an R package for comparing biological themes among gene clusters. OMICS 2012;16:284–7 [PubMed: 22455463]
25. Vassilev LT, Vu BT, Graves B, Carvajal D, Podlaski F, Filipovic Z, et al. In vivo activation of the p53 pathway by small-molecule antagonists of MDM2. Science 2004;303:844–8 [PubMed: 14704432]
26. Wang T, Yu H, Hughes NW, Liu B, Kendirli A, Klein K, et al. Gene Essentiality Profiling Reveals Gene Networks and Synthetic Lethal Interactions with Oncogenic Ras. Cell 2017;168:890–903e15 [PubMed: 28162770]
27. He L, Kulesskiy E, Saarela J, Turunen L, Wennerberg K, Aittokallio T, et al. Methods for High-throughput Drug Combination Screening and Synergy Scoring. Methods Mol Biol 2018;1711:351–98 [PubMed: 29344898]
28. Sun J, Wei Q, Zhou Y, Wang J, Liu Q, Xu H. A systematic analysis of FDA-approved anticancer drugs. BMC Syst Biol 2017;11:87 [PubMed: 28984210]
29. Hart T, Brown KR, Sircoulomb F, Rottapel R, Moffat J. Measuring error rates in genomic perturbation screens: gold standards for human functional genomics. Mol Syst Biol 2014;10:733 [PubMed: 24987113]

30. Jiang H, He X, Wang S, Jia J, Wan Y, Wang Y, et al. A microtubule-associated zinc finger protein, BuGZ, regulates mitotic chromosome alignment by ensuring Bub3 stability and kinetochore targeting. Dev Cell 2014;28:268–81 [PubMed: 24462186]
31. Yau EH, Kummetha IR, Lichinchi G, Tang R, Zhang Y, Rana TM. Genome-Wide CRISPR Screen for Essential Cell Growth Mediators in Mutant KRAS Colorectal Cancers. Cancer Res 2017;77:6330–9 [PubMed: 28954733]
32. Aguirre AJ, Meyers RM, Weir BA, Vazquez F, Zhang CZ, Ben-David U, et al. Genomic Copy Number Dictates a Gene-Independent Cell Response to CRISPR/Cas9 Targeting. Cancer Discov 2016;6:914–29 [PubMed: 27260156]
33. Munoz DM, Cassiani PJ, Li L, Billy E, Korn JM, Jones MD, et al. CRISPR Screens Provide a Comprehensive Assessment of Cancer Vulnerabilities but Generate False-Positive Hits for Highly Amplified Genomic Regions. Cancer Discov 2016;6:900–13 [PubMed: 27260157]
34. Mizuno H, Spike BT, Wahl GM, Levine AJ. Inactivation of p53 in breast cancers correlates with stem cell transcriptional signatures. Proc Natl Acad Sci U S A 2010;107:22745–50 [PubMed: 21149740]
35. Ben-Porath I, Thomson MW, Carey VJ, Ge R, Bell GW, Regev A, et al. An embryonic stem cell-like gene expression signature in poorly differentiated aggressive human tumors. Nat Genet 2008;40:499–507 [PubMed: 18443585]
36. Synold TW, Dussault I, Forman BM. The orphan nuclear receptor SXR coordinately regulates drug metabolism and efflux. Nat Med 2001;7:584–90 [PubMed: 11329060]
37. Housman G, Byler S, Heerboth S, Lapinska K, Longacre M, Snyder N, et al. Drug resistance in cancer: an overview. Cancers (Basel) 2014;6:1769–92 [PubMed: 25198391]
38. Torgovnick A, Schumacher B. DNA repair mechanisms in cancer development and therapy. Front Genet 2015;6:157 [PubMed: 25954303]
39. Lowe SW, Ruley HE, Jacks T, Housman DE. p53-dependent apoptosis modulates the cytotoxicity of anticancer agents. Cell 1993;74:957–67 [PubMed: 8402885]
40. Eischen CM. Genome Stability Requires p53. Cold Spring Harb Perspect Med 2016;6
41. Lanni JS, Jacks T. Characterization of the p53-dependent postmitotic checkpoint following spindle disruption. Mol Cell Biol 1998;18:1055–64 [PubMed: 9448003]
42. Tang YC, Williams BR, Siegel JJ, Amon A. Identification of aneuploidy-selective antiproliferation compounds. Cell 2011;144:499–512 [PubMed: 21315436]
43. Soto M, Raaijmakers JA, Bakker B, Spierings DCJ, Lansdorp PM, Foijer F, et al. p53 Prohibits Propagation of Chromosome Segregation Errors that Produce Structural Aneuploidies. Cell Rep 2017;19:2423–31 [PubMed: 28636931]
44. Weaver BA, Cleveland DW. Aneuploidy: instigator and inhibitor of tumorigenesis. Cancer Res 2007;67:10103–5 [PubMed: 17974949]
45. Saatci O, Borgoni S, Akbulut O, Durmus S, Raza U, Eyupoglu E, et al. Targeting PLK1 overcomes T-DM1 resistance via CDK1-dependent phosphorylation and inactivation of Bcl-2/xL in HER2-positive breast cancer. Oncogene 2018;37:2251–69 [PubMed: 29391599]
46. Higuchi F, Fink AL, Kiyokawa J, Miller JJ, Koerner MVA, Cahill DP, et al. PLK1 inhibition targets Myc-activated malignant glioma cells irrespective of mismatch repair deficiency-mediated acquired resistance to temozolomide. Mol Cancer Ther 2018
47. Sur S, Pagliarini R, Bunz F, Rago C, Diaz LA Jr., Kinzler KW, et al. A panel of isogenic human cancer cells suggests a therapeutic approach for cancers with inactivated p53. Proc Natl Acad Sci U S A 2009;106:3964–9 [PubMed: 19225112]
48. Kops GJ, Foltz DR, Cleveland DW. Lethality to human cancer cells through massive chromosome loss by inhibition of the mitotic checkpoint. Proc Natl Acad Sci U S A 2004;101:8699–704 [PubMed: 15159543]
49. Michel L, Diaz-Rodriguez E, Narayan G, Hernando E, Murty VV, Benezra R. Complete loss of the tumor suppressor MAD2 causes premature cyclin B degradation and mitotic failure in human somatic cells. Proc Natl Acad Sci U S A 2004;101:4459–64 [PubMed: 15070740]
50. McGranahan N, Swanton C. Clonal Heterogeneity and Tumor Evolution: Past, Present, and the Future. Cell 2017;168:613–28 [PubMed: 28187284]

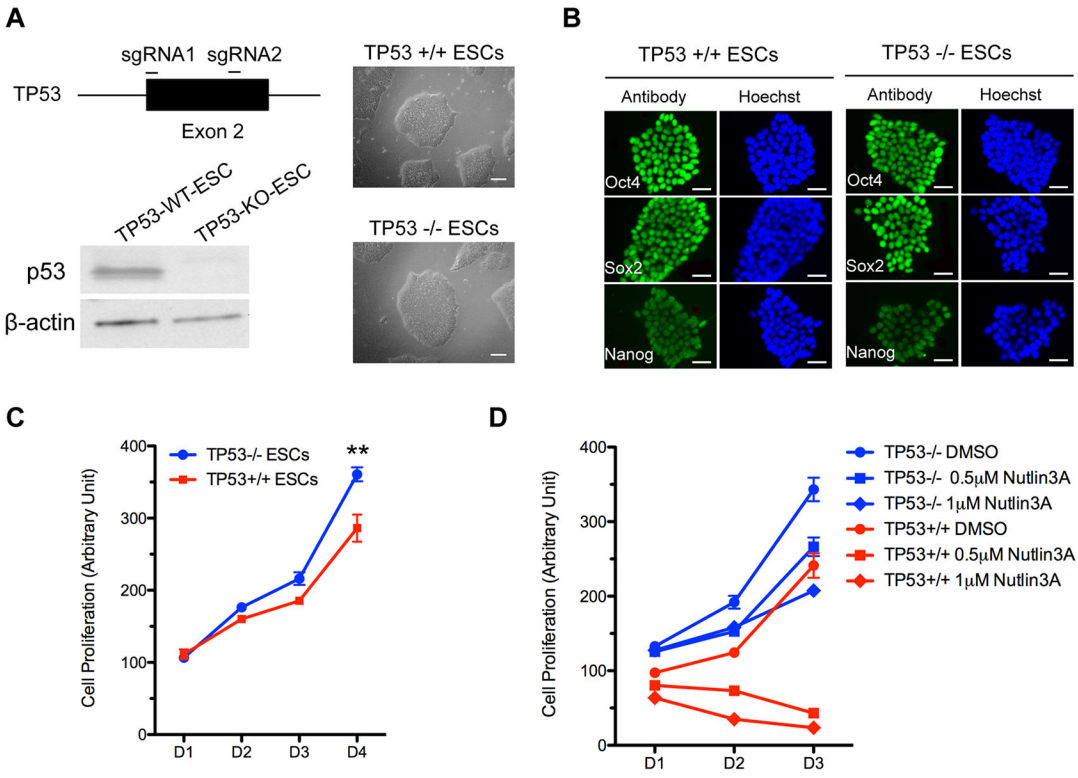

Figure 1. Generation of TP53 knockout human embryonic stem cell line with CRISPR-Cas9 gene editing system.

A, Left panel top: TP53 sgRNAs location; Bottom: Western blotting result showing p53 expression was abolished by TP53 knockout; Right panel: Representative images of morphology of TP53-KO and TP53-WT human H9 ES cells, scale bar: 1000 um. **B**, Representative images for immunostaining of TP53-KO and TP53-WT human ESCs pluripotent markers Oct4, Sox2, and Nanog. Nuclei are visualized with Hoechst staining, scale bar: 200 um. **C**, Cell proliferation of TP53-KO and TP53-WT human ESCs were determined by resazurin at different day as indicated. **, $p < 0.01$. **D**, Functional p53 test for TP53-KO human ESCs using Nutlin-3a that could accumulate p53 in cells by inhibiting MDM2 interaction with p53 protein.

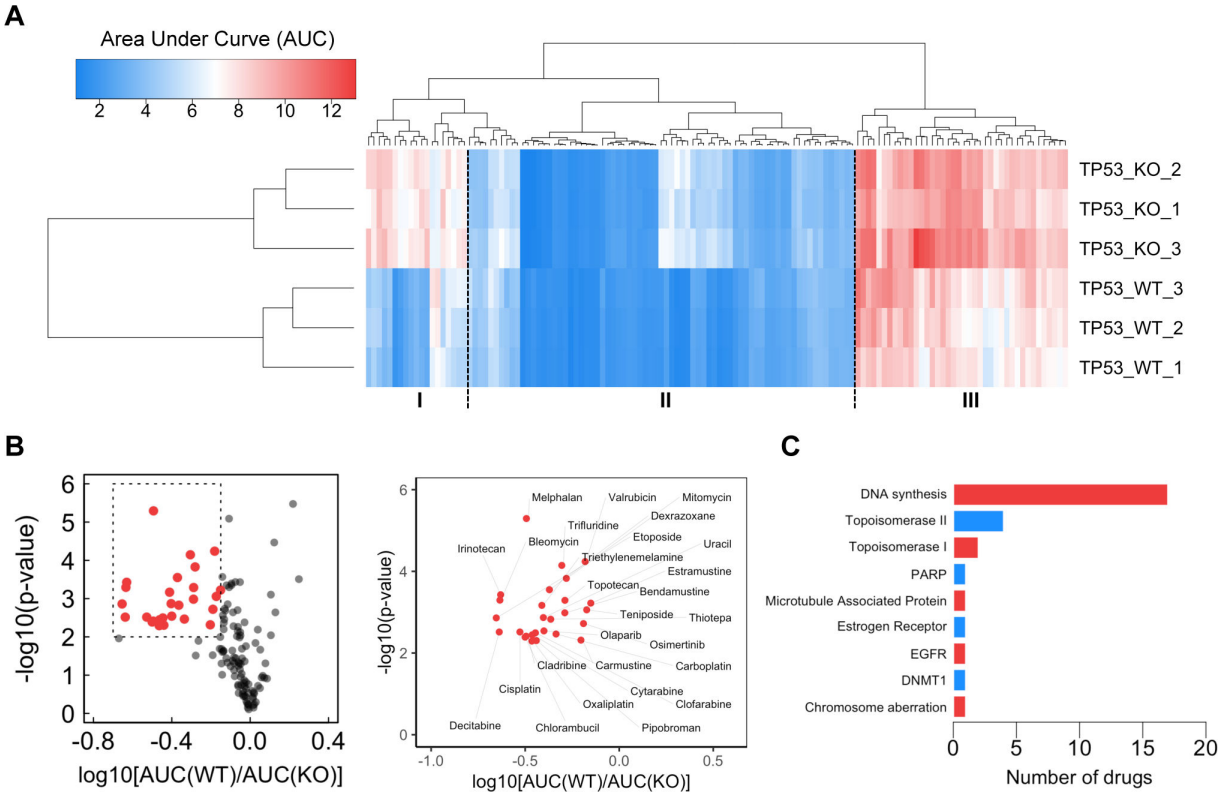

Figure 2. A systematic screen of FDA approved drugs in TP53-WT versus TP53-KO hESCs.

A, The heatmap of area under curve (AUC) for all drugs screening in this study. **B**, Scatter plot of drugs screening. Left panel: A volcano plot representation of student's t-test results shows the magnitude (The log10 of ratio between AUC of TP53-WT and of TP53-KO, x-axis) and significance (p value, y-axis) of all drug-TP53 associations. Each dot represents a single drug and red dots indicate the drugs were statistical significance between AUC of TP53-WT and TP53-KO, p value < 0.01. Right: Scatter plot is magnified views of p53-null hESCs resistant drugs and the drug names are showing. **C**, The panel of 27 p53-null hESCs resistant drugs classified according to their therapeutic targets. A single drug may be included in multiple categories.

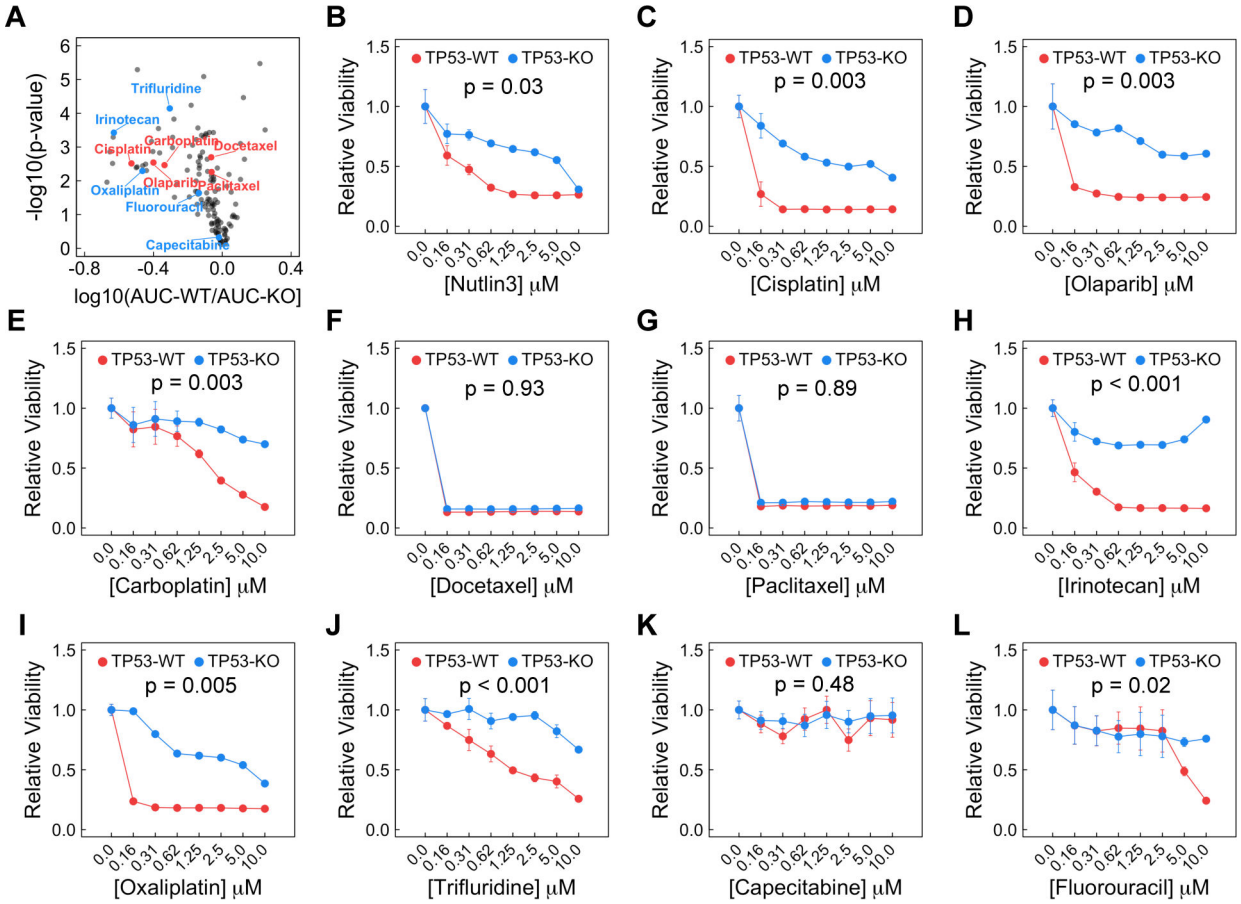

Figure 3. Validation of drugs for colorectal cancer and epithelial ovarian cancer chemotherapy.

A, A volcano plot representation of student's t-test results on AUC shows the magnitude and significance of all drug-TP53 associations. The name of common drugs for colorectal cancer and epithelial ovarian cancer chemotherapy were showing. **B**, Viability of TP53-WT and TP53-KO hESCs after Nutlin-3a treatment as a positive control. **C-L**, Viability of TP53-WT and TP53-KO hESCs that were treated with different drugs respectively. P values from two-tailed student's t test on AUC were showed on plots.

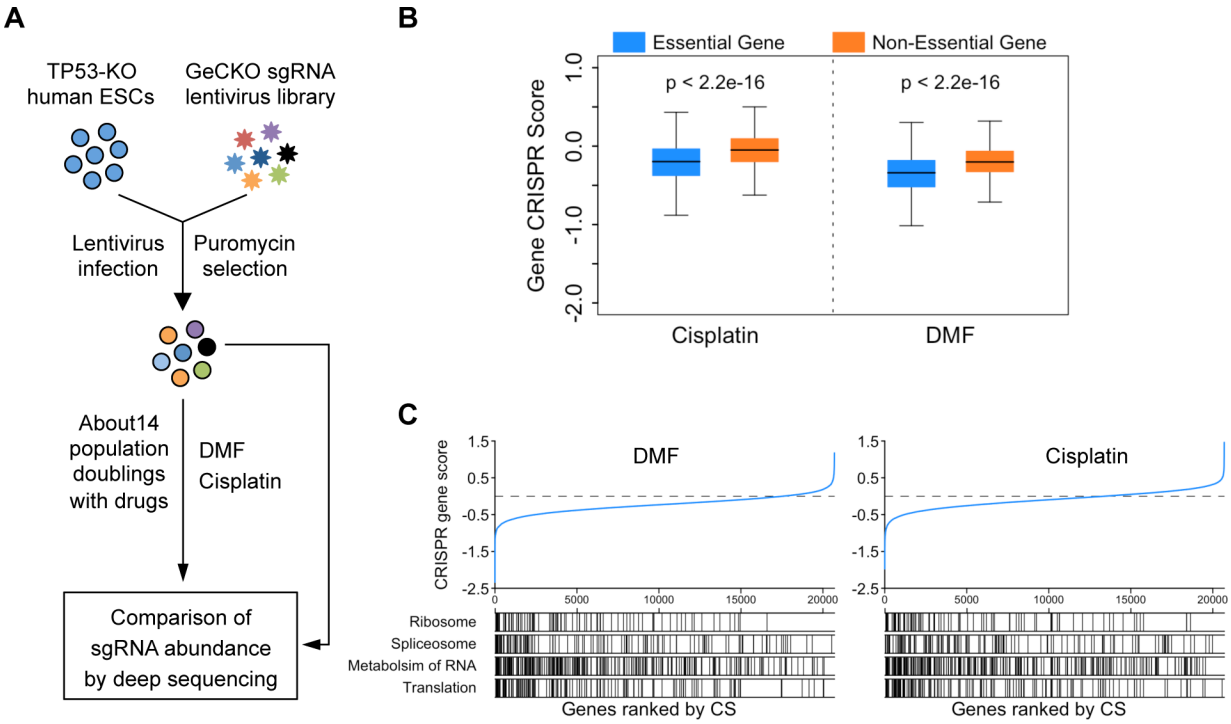

Figure 4. Genome-wide CRISPRs screening on TP53-KO hESCs with or without drugs.

A, Workflow of genome-scale CRISPR screening on TP53-KO hESCs with drugs. **B**, Boxplot of CRISPR gene scores of 927 non-essential genes and 1,580 essential fitness genes in Cisplatin and DMF treatment. P values between gene CRISPR score of essential genes and nonessential genes were from student's t test. **C**, Gene sets enrichment analysis of essential biological process of cell proliferation in DMF treatment TP53-KO hESCs and Cisplatin treatment TP53-KO hESCs.

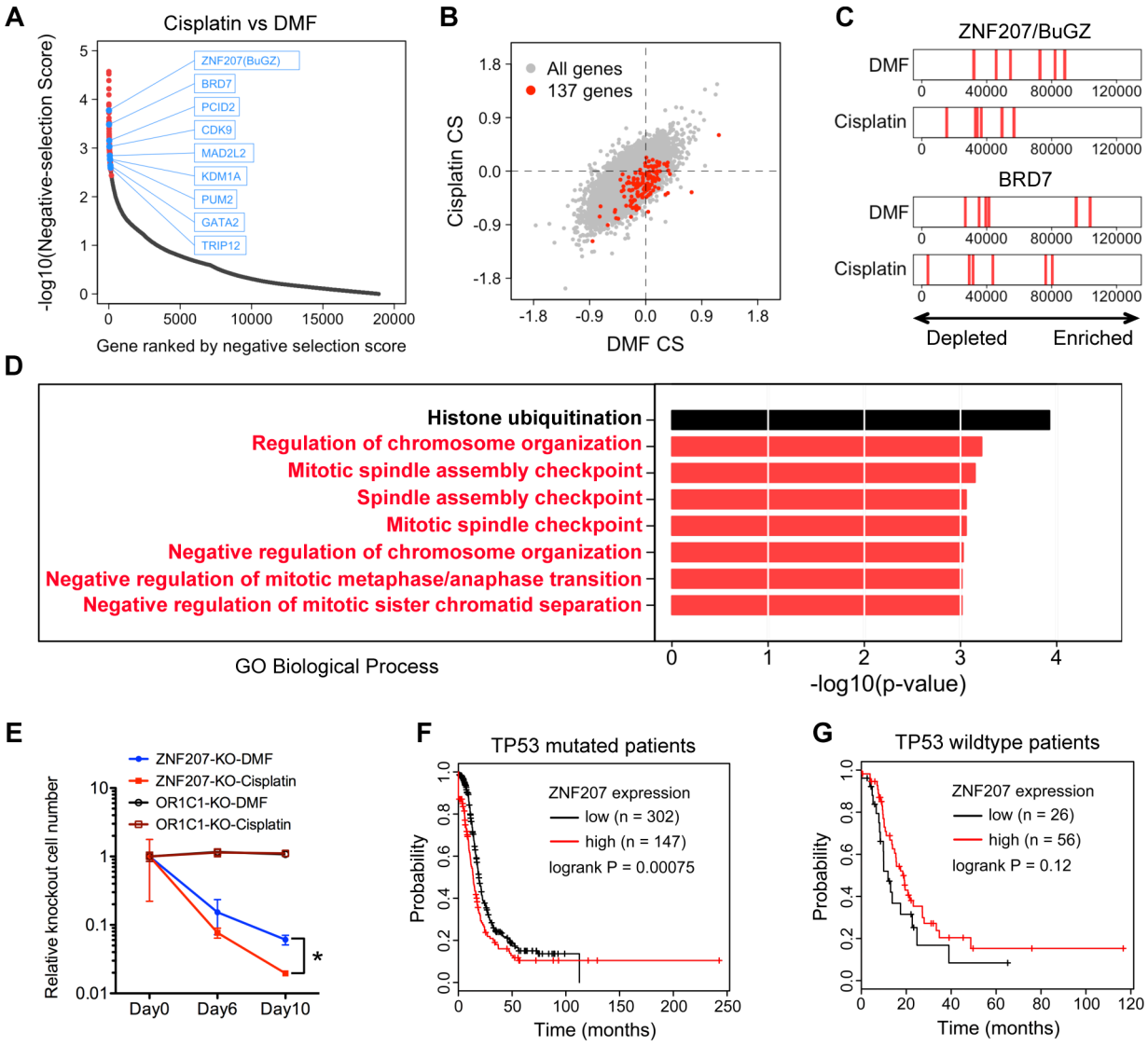

Figure 5. Candidates that could re-sensitize human ESCs to Cisplatin.

A, Gene rank ordered by negative selection score from MAGeCK output from Cisplatin treatment versus DMF. Red dots: significant genes between Cisplatin treatment and DMF control ($p < 0.01$) from MAGeCK analysis. Blue dots: genes involving in spindle assembly checkpoint and chromosome organization. **B**, Scatterplots of CRISPR gene scores of Cisplatin treated TP53-KO hESCs and DMF treated TP53-KO hESCs. Grey dot: all genes. Red dot: the 137 significant genes between Cisplatin treatment and DMF treatment from MAGeCK software. **C**, The position of 6 sgRNAs targeting gene ZNF207/BuGZ or BRD7 are showing in ordered rank of all library sgRNA counts. Red line: sgRNAs targeting the same gene. **D**, Top eight GO biological processes of GO analysis for 137 significant genes. **E**, Cas9-expressed TP53-KO human ESCs were infected with ZNF207/BuGZ sgRNAs or control OR1C1 sgRNAs. Then treated with DMF and Cisplatin, respectively. The ZNF207/BuGZ or OR1C1 knockout cells were monitored by qPCR. *, $p < 0.05$. Kaplan-Meier survival plot was generated from the cohort of ovarian cancer patients according to ZNF207

expression level (http://kmplot.com/analysis/). P values on the plots are from log-rank test for the comparisons of the low and high ZNF207 expression groups. **F**, All 449 patients are TP53-mutated and received chemotherapy that contained platin. **G**, All 82 patients are TP53-wt and received chemotherapy that contained platin.

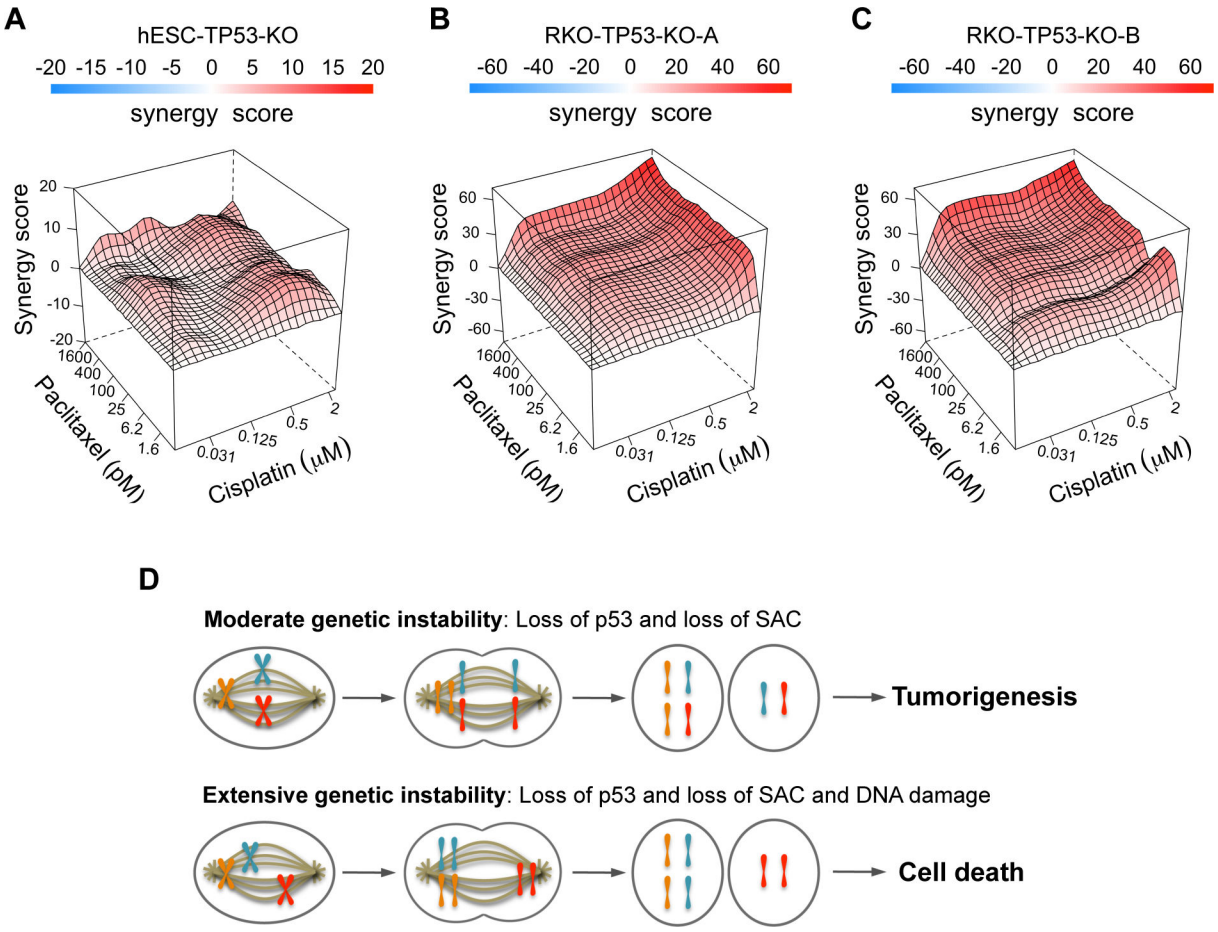

Figure 6. Chromosome missegregation by Paclitaxel could sensitize TP53-KO hESCs and TP53-KO colon cancer cells to Cisplatin.

The 3D plotting shows average synergy score of Paclitaxel and Cisplatin from three 96-well plates on TP53-KO hESCs (**A**), RKO colon cancer cells TP53-KO-A (**B**) and RKO colon cancer cells TP53-KO-B (**C**). **D**, A predicted model of Cisplatin cause cell death with dysregulation of chromosome segregation. Moderate levels of genetic instability, caused by mutations in mismatch repair genes or by missegregation of one to three chromosomes per division promote cell growth and tumorigenesis (top panel). High levels of genetic instability, caused by chemotherapeutic agents such as Cisplatin or missegregation of large numbers of chromosomes per division, result in cell death and tumor suppression (low panel).

Table 1.

Top 20 GO terms of gene sets enrichment analysis

GO ID	Description	p-value
GO:0016574	Histone ubiquitination	0.000118963
GO:0033044	Regulation of chromosome organization	0.000604182
GO:0007094	Mitotic spindle assembly checkpoint	0.000707993
GO:0071173	Spindle assembly checkpoint	0.00087609
GO:0071174	Mitotic spindle checkpoint	0.00087609
GO:2001251	Negative regulation of chromosome organization	0.000943002
GO:0045841	Negative regulation of mitotic metaphase/anaphase transition	0.000968826
GO:2000816	Negative regulation of mitotic sister chromatid separation	0.000968826
GO:1902100	Negative regulation of metaphase/anaphase transition of cell cycle	0.001067552
GO:1905819	Negative regulation of chromosome separation	0.001067552
GO:0045995	Regulation of embryonic development	0.001141201
GO:0033048	Negative regulation of mitotic sister chromatid segregation	0.001172416
GO:2000177	Regulation of neural precursor cell proliferation	0.001396664
GO:0033046	Negative regulation of sister chromatid segregation	0.001401117
GO:0051985	Negative regulation of chromosome segregation	0.001525227
GO:0061351	Neural precursor cell proliferation	0.001573555
GO:0031056	Regulation of histone modification	0.001628104
GO:0031577	Spindle checkpoint	0.001656022
GO:0010948	Negative regulation of cell cycle process	0.002015403
GO:0051983	Regulation of chromosome segregation	0.002132651